Utilizing machine learning algorithm, cloud computing platform and remote sensing satellite data for impact assessment of flood on agriculture land

Himanshu Kumar[1,2,*], Rohan Kumar[2], Sujay Dutta[3], Magan Singh[1] and Sateesh Kr. Karwariya[4]

[1]ICAR-National Dairy Research Institute, Karnal 132 001, India
[2]Lovely Professional University, Phagwara 144 001, India
[3]Space Applications Centre, Indian Space Research Organizations, Ahmedabad 380 015, India
[4]Commissionerate of Rural Development, Government of Gujarat, Gandhinagar 382 010, India

Floods are one of the most devastating natural disasters that cause immense damage to life, property and agriculture worldwide. Recurring floods in Bihar (a state in eastern India) during the monsoon season impact the agro-based economy, destroying crops and making it difficult for farmers to prepare for the next season. To mitigate the impact of floods on the agricultural sector, there is a need for early warning systems. Nowadays, remote sensing technology is used extensively for monitoring and managing flood events, which is also used in the present study. The random forest (RF) machine learning (ML) algorithm has also been used for land-use classification, and its output is used as an input for flood impact assessment. Here, we have analysed the flood extents and their impact on agriculture using Sentinel-1 SAR, Sentinel-2 and Planet Scope optical imageries on the Google Earth Engine (GEE) cloud computing platform. The present study shows that floods severely impacted a large part of Bihar during the monsoon seasons of 2020 and 2021. About 701,967 ha of land (614,706 ha agricultural land) in 2020 and 955,897 ha (851,663 ha agricultural land) in 2021 were severely flooded. An inundation maps and area statistics have been generated to visualise the results, which can help the government authorities prioritize relief and rescue operations.

Keywords: Agriculture, cloud computing platforms, floods, machine learning algorithm, remote sensing data.

FLOOD is a major natural disaster in the Indian state of Bihar, which severely impacts the property, infrastructure and agriculture every year. Rapid urban growth, deforestation, unplanned development and erratic rainfall are the main causes of frequent floods in North Bihar, mostly during the monsoon season. Due to overflowing rivers in the neighbouring country of Nepal, North Bihar has experienced severe floods during the past three decades[1,2]. The COVID-19 pandemic has worsened the situation, where natural disasters and other factors have disrupted the economic and social stability of communities. Floods significantly impact the agricultural sector, which is the major source of livelihood for many people in Bihar. When floods occur, crops are completely destroyed, making it difficult for the farmers to earn a living. Additionally, floods damage homes and other infrastructure, making it unsafe to live. As a result, many people in North Bihar are forced to migrate to other areas in search of work during floods to sustain their lives. It is a difficult and often traumatic experience, as families are separated, and individuals are forced to leave their homes and communities behind.

To mitigate the impact of floods, an early warning system is needed in Bihar. Hence, the use of remote sensing and geospatial technology, in addition to hydrological data for flood extent mapping and monitoring, is important for mitigating the impact of floods in Bihar. Remote sensing technology is capable to provide data on rainfall, water level and soil moisture, which can provide valuable information for farmers and local authorities to take preventive measures for floods.

Synthetic aperture radar (SAR) data is more effective than multi-spectral optical datasets for flood mapping and monitoring due to its all-weather sensing capability. The European Space Agency (ESA) launched the Sentinel-1A satellite on 3 April 2014 and Sentinel-1B on 25 April 2016 for SAR data. Its revisit time is six days at the equator with two satellites (Sentinel-1A/B)[3]. Nowadays, the remotely sensed earth observation (EO) datasets are commonly used for disaster management[4] and are freely available to researchers. However, these datasets are computationally and storage-intensive data types. Users must have high-performance computers and large amounts of storage space to download, store and process the data. To resolve these complications, Google has launched the most advanced cloud-based geo-computing platform, viz. 'Google Earth

*For correspondence. (e-mail: himanshukumar.gis@gmail.com)

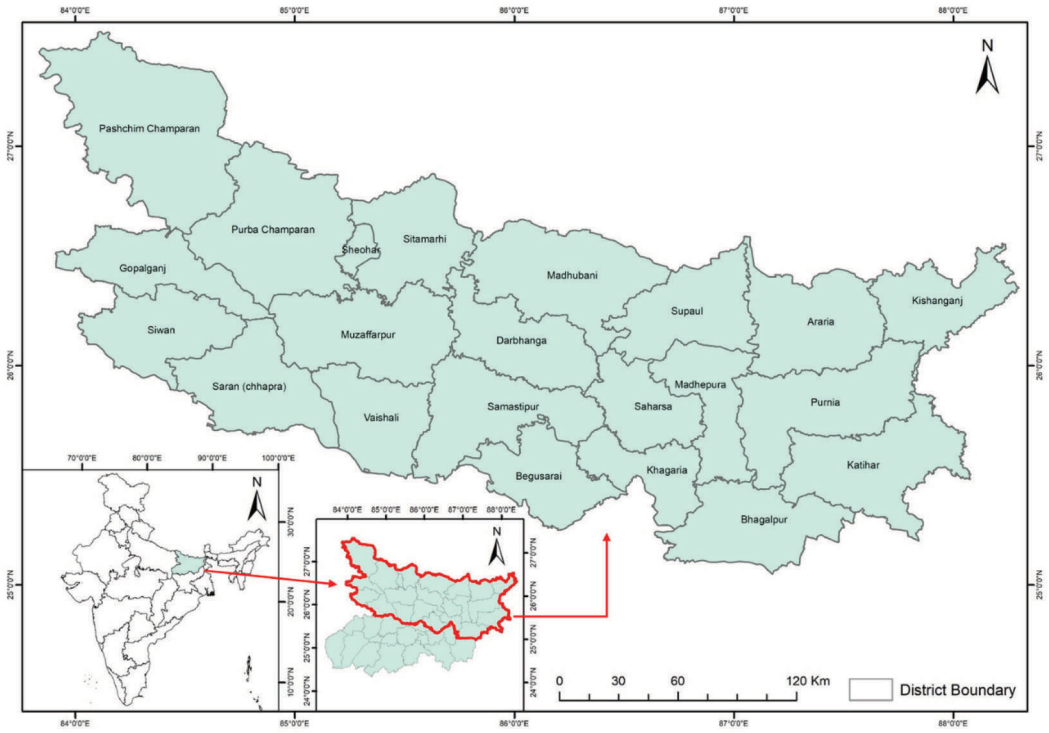

Figure 1. Location map of the study area.

Engine (GEE)'. This platform enables us to process huge satellite datasets without requiring local storage[5].

In the present study, Sentinel-2 MSI and PLANET-NICFI (PlanetScope) optical datasets have been utilized for land-use/land-cover (LU/LC) mapping and Sentinel-1 SAR for flood extent mapping and monitoring. The ability of SAR sensors to detect the extent of flooding depends on different scattering mechanisms. Inundated pixels can be identified using several methods that rely on the scattering mechanism. These methods apply backscatter thresholds to the imagery to differentiate between inundated and non-inundated areas[6]. Usually, the change detection technique is utilized to identify flooded pixels using SAR datasets.

Likewise, various methods and indices exist to extract waterbodies using optical and microwave satellite datasets. The Normalized Difference Water Index (NDWI) was proposed by McFeeters[7] in 1996 and has been shown to be a robust index for detecting waterbodies, especially in areas with high vegetation cover. The Modified Normalized Difference Water Index (MNDWI) was proposed by Xu[8] in 2006 as a modification of NDWI, specifically designed for urban areas. It effectively extracts waterbodies in urban areas with high reflectance from built-up structures. The Automated Water Extraction Index (AWEI) was developed by Feyisa *et al.*[9] in 2014. It is designed to overcome the limitations of NDWI and MNDWI in areas with mixed pixels, such as rivers or wetlands. AWEI is based on a combination of the green, blue, and red bands, as well as the shortwave infrared and thermal infrared bands, allowing for more accurate detection of waterbodies. These indices have been widely used and validated for detecting water bodies and assessing the impact of floods. The threshold technique is also used to identify flood extent using JavaScript code. Therefore, it is always necessary to have accurate data on flooded areas for an accurate assessment of the damage in order to make a viable decision on prioritizing relief.

Several studies have been undertaken over the years to deal with the consequences of frequent floods in Bihar, using optical and SAR satellite datasets[10–14]. However, limited studies have been conducted regarding the effects of floods on agriculture utilizing cutting-edge technology like machine learning (ML) algorithms, high-resolution satellite data (such as Sentinel-1 and 2 and PlanetScope) and cloud computing platforms like GEE.

The present study aims to address the existing research gap by incorporating these advanced approaches, which offer faster flood extent demarcation and map generation capabilities. Additionally, this study leverages the combined power (data fusion) of Sentinel-2 and PlanetScope satellite datasets for precise land-use classification using ML approaches.

Materials and methods

Study area

This study was carried out in North Bihar (24.33611–27.52083 N lat. and 83.33055–88.29444 E long.; Figure 1). According to the Census of India 2011, Bihar has a population of 10.41 crores[15]. The state receives 1205 mm of rainfall

Table 1. Datasets used in the study

Data	Duration	Resolution (m)	Source	Aim	Assessing path
Sentinel-1A/B SAR	June to October (2020 and 2021)	10	European Space Agency (ESA)	To demarcate flooded regions and flooded agricultural fields	COPNERICUS/S1
Sentinel-2A/B optical	March (2020 and 2021)			Land-use mapping	COPNERICUS/S2
PLANET-NICFI (PlanetScope)	March (2020 and 2021)	4.77	ESA		Planet-nicfi/assets/basemaps
Shuttle Radar Topography Mission	2000	30	NASA	Terrain correction	SRTMGL1_003

Box 1. Syntax/code.

Resample the Sentinel-2 10 m band to PlanetScope 4.77 m using bilinear interpolation method

```
var resampled
=image.select(bands).
resample('bilinear')
.reproject(proj4.77m);
```

each year on average and has the world's most fertile alluvial plains of the Gangetic Valley. Its soil distribution is loam, clay, clay loam and sandy loam[16]. The main agricultural products of Bihar include maize, wheat and rice. The present study considered 22 districts of Bihar. North Bihar is home to several rivers responsible for recurrent flooding in the region. The major rivers include the Kosi, Gandak, Budhi Gandak, Bagmati and Mahananda. In the past, these rivers caused devastating floods in the state, with North Bihar being the worst affected. The Kosi River, which runs through Bihar, is known as the 'Sorrow of Bihar' owing to its unpredictable and destructive floods.

Data used

In this study, major emphasis has been given on the capabilities of multi-source remote sensing data (Table 1) in assessing the impact of floods on agriculture in North Bihar.

Sentinel-1 SAR: The openly accessible Sentinel-1 SAR datasets offered by ESA have been utilized in the present study. The interferometric wide swath (IW) mode has been used due to its conflict-free nature and the availability of both vertical transmit–vertical receive (VV) and vertical transmit–horizontal receive (VH) polarization. The SNAP tool package has been used to process satellite data for noise removal, radiometric, orbital and terrain corrections by SRTM datasets. In this study, all the accessible Sentinel-1 SAR datasets have been utilized for flood mapping and monitoring purposes.

Sentinel-2A/B MSI: Freely accessible Sentinel-2A/B Multispectral Instrument (MSI) satellite datasets can monitor the land surface. The revisit frequency of this satellite is ten days with a single satellite and five days with combined/dual satellites. In this study, we utilized bands 2, 3, 4 and 8 of the Sentinel-2 dataset for land-use mapping.

NICFI (PlanetScope): In collaboration with Google and Norway's International Climate and Forest Initiative (NICFI), the high-resolution composite base maps of PlanetScope for tropical regions have recently become accessible within GEE[17]. Its spatial resolution is 4.77 m, with four bands, viz. blue, green, red and NIR. This dataset is available from 2015 to 2020 as base map composites of 3 and 6 months, and as a monthly composite since September 2020 (ref. 18). We have used datasets from March 2020 and 2021 for land-use mapping.

Methodology

Harmonization of PlanetScope and Sentinel-2A/B MSI: Bilinear interpolation is a widely used method for resampling images[19,20]. In this study, the bilinear interpolation method has been used in the GEE platform to adjust the resolution of the Sentinel-2 dataset and match it to the 4.77 m resolution of PlanetScope (Box 1). We have utilized bands blue, green, red and NIR of PlanetScope and Sentinel-2A/B MSI for land-use mapping.

The land-use map has been prepared using harmonized Sentinel-2 MSI and PlanetScope datasets for extracting flooded agriculture lands of 2020 and 2021. Otsu automatic thresholding technique was used for the identification of inundated pixels[21–24]. An automated thresholding approach can detect threshold values to distinguish water pixels from other pixels without having any training sample datasets[25,26]. Presently, the threshold value is equal to or less than –3 dB used for flood. The pre-flood layer of water bodies was deducted from the obtained flood extent to get the final result. Figure 2 is a flowchart showing the methodology used in this study.

Google Earth engine: SAR data processing is a complex task that requires separate computational systems and storage space along with specialized software. However, GEE provides a unique solution to these challenges through a cloud-based platform that allows users to process the datasets.

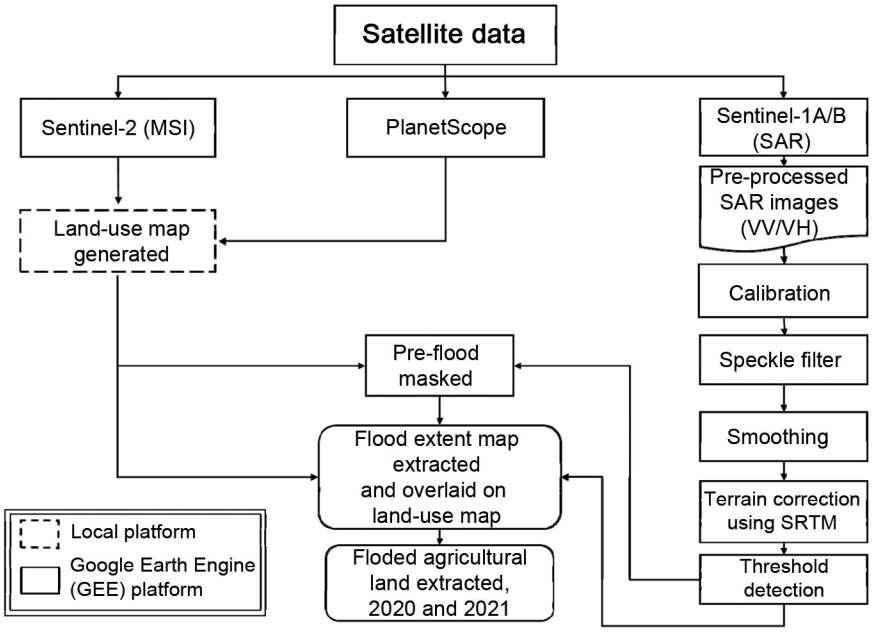

Figure 2. Methodology.

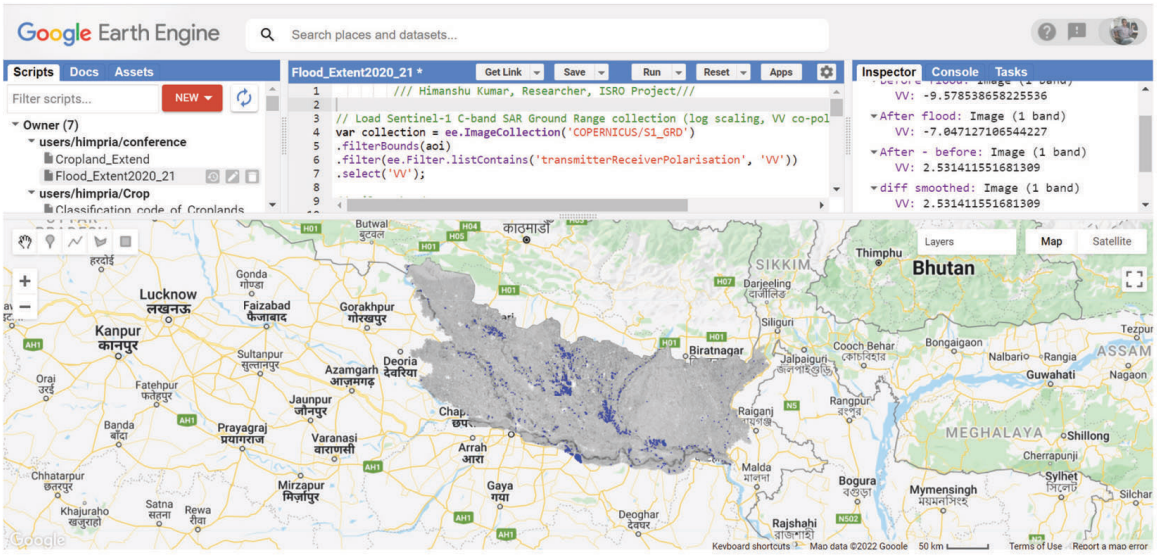

Figure 3. Interface of cloud computing platform of Google Earth Engine.

The GEE platform provides access to vast satellite imagery, including SAR data, which can be processed in real-time or near-real-time. We have used the GEE cloud computing platform for the entire analysis. A web-based IDE code was developed (https://code.earthengine.google.com/?scriptPath=users%2F%2F%3AFlood_Extent2020_21_NB) for estimation of flood extents and impacted agricultural lands (Figure 3).

Random forest classifier: The random forest classifier (RFC) is an ML algorithm commonly used for image classification including land-use map preparation utilizing remote sensing data. In this context, Sentinel-2 and PlanetScope data are often used as inputs to the algorithm. Initially, 110 trees were used in the RF model in this study (Syntax: ee.Classifier.smileRandomForest (110)). RFC works by generating multiple decision trees, each of which predicts the land use class of a pixel based on its spectral properties (Figure 4). The algorithm then combines the results of these decision trees to produce a final classification map. This classifier is commonly used due to its capability to handle complex spectral interactions and nonlinear relationships between the spectral bands and land-use classes, making it a powerful tool for image classification.

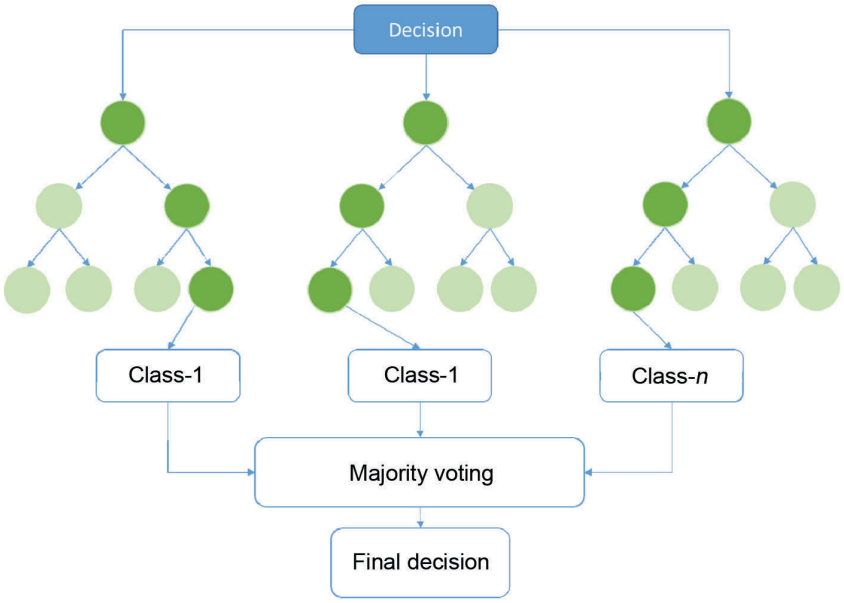

Figure 4. Random forest classifier flowchart.

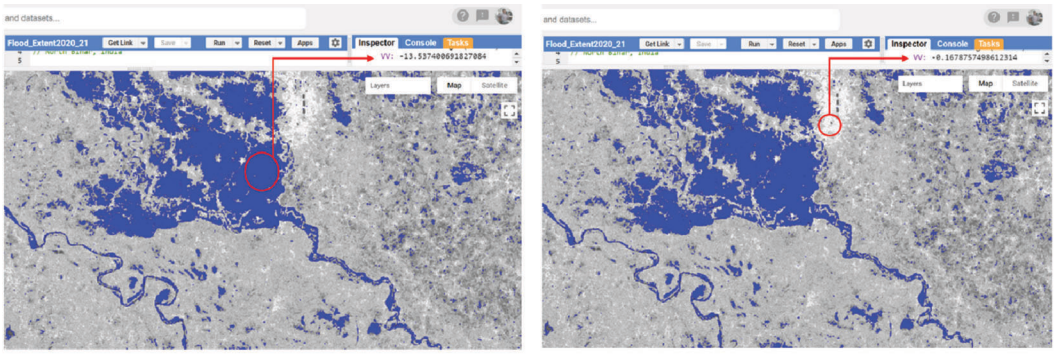

Figure 5. Backscatter intensity of pixels.

In the present study, Sentinel-2 and PlanetScope data have been used together for land-use mapping, which allows for a more comprehensive view of the Earth's surface. The Sentinel-2 data provide broad spectral coverage, allowing for identifying a wide range of land-cover types. The PlanetScope data provide high-resolution imagery, which allows for identifying smaller features on the Earth's surface. The land-use map generated by RFC was utilized in the study for flood impact assessment.

Results and discussion

Backscatter intensity of flooded pixels

The intensity of the backscatter pattern of the processed microwave (SAR) Sentinel-1 dataset is influenced by several factors, such as roughness, slope, moisture content and vegetation cover of the surface. For instance, a smooth surface like water reflects less radar energy and produces a dark backscatter pattern, while a rough surface like mountainous terrain reflects more radar energy and produces a bright backscatter pattern. Thus, the intensity of the backscatter pattern can provide information about the types of features present on the Earth's surface, such as water bodies, forests, urban areas and agricultural land.

In the present study, pixels having low grey-scale intensity represent waterbodies and features, while high-intensity pixels represent human-made or non-water features[5]. We have used VV polarization in this study. The backscatter intensity has been measured in decibels (Figure 5).

Flood impact analysis

An analysis was conducted to assess the impact of floods in North Bihar. For this, satellite images from March 2020 were used to identify pre-flood conditions, while images

Table 2. District-wise flood-affected areas extracted using Sentinel-2 and PlanetScope data

Flooded districts in Bihar	Geographical area (ha)	Total flood affected area (ha^{-1})		Flood affected area (%)		Change (%)	Total flood affected agricultural land (ha^{-1})		Total population	Flood-affected population	
		2020	2021	2020	2021		2020	2021		2020	2021
Arariya	279,704.17	3947.74	44,483.00	1.41	15.90	14.49	3441.74	43,340.00	2,806,200.00	39,607	446,287
Begusarai	193,309.07	25.00	40,811.00	1.29	21.11	19.82	0.00	37,915.00	2,954,367.00	38,111	623,720
Bhagalpur	255,331.10	42,244.77	86,790.00	16.55	33.99	17.45	34,112.77	76,829.00	3,032,226.00	501,685	10,30,689
Darbhanga	250,777.93	88,383.58	78,003.00	35.24	31.10	–4.14	84,302.58	73,628.00	3,921,971.00	1,382,250	1,219,906
Gopalganj	204,110.19	26,793.86	11,290.00	13.13	5.53	–7.60	22,462.86	8867.00	2,558,037.00	335,798	141,493
Katihar	303,561.68	48,795.21	81,420.00	16.07	26.82	10.75	40,255.21	68,816.00	3,068,149.00	493,181	822,926
Khagaria	149,187.39	37,009.35	51,667.00	24.81	34.63	9.82	35,361.35	49,774.00	1,657,599.00	411,205	574,064
Kishanganj	198,830.24	3597.59	21,873.00	1.81	11.00	9.19	2903.59	20,594.00	1,690,948.00	30,596	186,019
Madhepura	180,027.66	27,470.43	29,620.00	15.26	16.45	1.19	23,587.43	26,133.00	1,994,618.00	304,359	328,175
Madubani	350,145.84	31,718.79	49,118.00	9.06	14.03	4.97	30,583.79	48,013.00	44,76,044.00	405,473	627,894
Muzaffarpur	317,792.18	70,620.01	68,351.00	22.22	21.51	–0.71	62,583.01	60,480.00	4,778,610.00	1,061,906	1,027,787
Pachim Champaran	523,841.15	35,093.54	28,461.00	6.70	5.43	–1.27	26,583.54	19,256.00	3,922,780.00	262,798	213,130
Purba Champaran	397,076.47	76,045.16	56,278.00	19.15	14.17	–4.98	67,483.16	49,819.00	5,082,868.00	973,433	720,399
Purnia	321,126.64	24,183.87	57,396.00	7.53	17.87	10.34	20,368.87	51,827.00	3,273,127.00	246,497	585,017
Saharsa	166,419.72	38,150.54	29,208.00	22.92	17.55	–5.37	33,951.54	25,706.00	1,897,102.00	434,897	332,957
Samastipur	268,545.22	25,867.16	61,176.00	9.63	22.78	13.15	23,895.16	58,048.00	4,254,782.00	409,835	969,262
Saran	267,895.35	32,303.37	40,353.00	12.06	15.06	3.00	27,047.37	34,639.00	3,943,098.00	475,467	593,948
Sheohar	44,185.79	4845.21	2970.00	10.97	6.72	–4.24	4770.21	2903.00	656,916.00	72,034	44,155
Sitamarhi	218,858.48	32,173.55	23,434.00	14.70	10.71	–3.99	30,813.55	22,306.00	3,419,622.00	502,705	366,152
Siwan	221,989.66	31,425.75	8163.00	14.16	3.68	–10.48	26,767.75	5312.00	3,318,176.00	469,734	122,016
Supaul	241,658.20	8536.27	35,178.00	3.53	14.56	11.02	5149.27	28,788.00	2,228,397.00	78,715	324,386
Vaishali	202,102.12	12,736.51	49,854.00	6.30	24.67	18.37	8281.51	38,670.00	3,495,249.00	220,271	862,198
	5,556,476.26	701,967.26	955,897.00	12.63	17.20	4.57	614,706.26	851,663.00	68,430,886.00	91,50,559	11,772,367

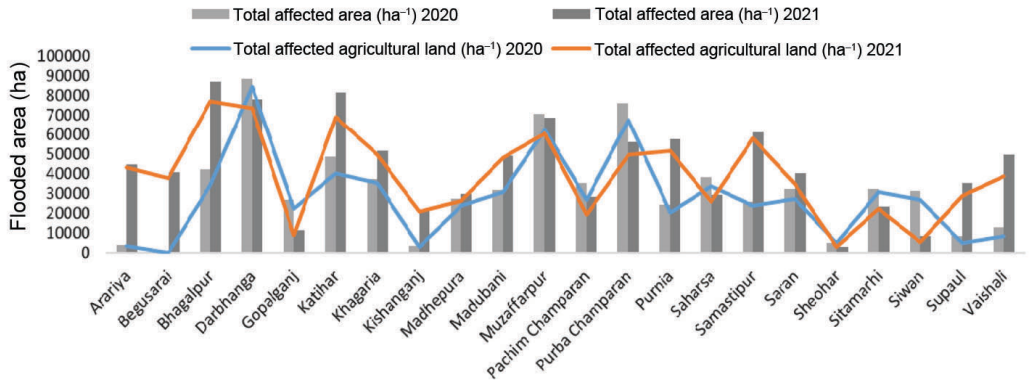

Figure 6. District-wise flood statistics.

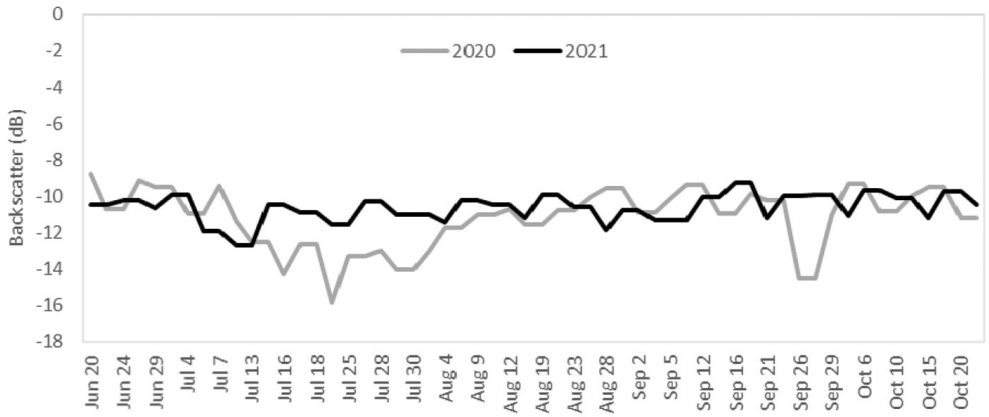

Figure 7. Backscatter response of VV polarization in 2020 and 2021.

from June to October in both 2020 and 2021 were used to identify peak flood events. By subtracting the pre-flood layer from the peak-flood layer, the actual flood extent was derived. To determine the affected areas and population (Table 2), the boundaries of villages, blocks and districts provided by the Survey of India (having population data in the attribute table) were overlaid on the actual flood extent map.

It is reported that about 22 districts in Bihar are on high alert during monsoon season every year[27,28]. This is because these districts are situated in the basins of Kosi, Ganga, Gandak and Mahanadi, which overflow every year due to heavy rainfall. The analysis indicates that almost 701,942 ha area (about 21 districts) in 2020 and 955,897.00 ha (about 22 districts) in 2021 of North Bihar were flooded. The worst affected districts in 2020 were Darbhanga, Muzaffarpur, West Champaran, Saran and Siwan. In 2021, Bhagalpur, Darbhanga, Muzaffarpur, West Champaran, Katihar, Vaishali and Khagaria districts were severely affected by floods (Figure 6). In 2020 and 2021, floods submerged over 614,706.26 and 851,663 hectares of agricultural land, respectively. The majority of Bihar's population relies on agriculture for its livelihood, which is the sector that suffers maximum damage from recurrent floods.

Flood progression evaluation using Sentinel-1 SAR data

In this study, VV polarization has been utilized for flood extent mapping, wherein the backscatter response of VV ranges between –8 and –16 dB (Figure 7). We found that high values of VV represent non-water features, while water bodies represent low backscatter responses.

Pre-flood land-use map

Land-use mapping involves using remote sensing data to identify and classify different types of land cover such as 'forests, croplands, urban areas and water bodies'. Environmental managers, urban planners and policymakers often use this information to make quick decisions about how to use and manage the land. In the present study, Sentinel-2A/B (<10% clouded data) and PlanetScope images were used to extract land-use maps using RF method on GEE cloud computing platform. A pre-flood land-use map was used (Figure 8), and the flood extent was overlaid to identify land use impacted by floods in 2020 and 2021.

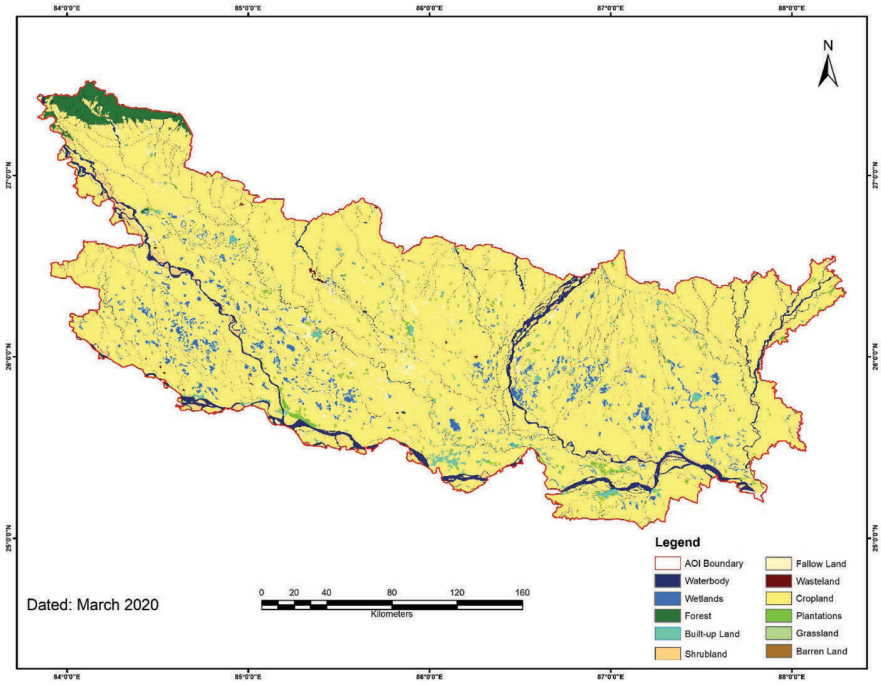

Figure 8. Land-use map of pre-flood area.

Flood 2020

The analysis showed that several districts in Bihar were severely affected by floods in 2020. More than 8000 ha of cropland in Darbhanga, East Champaran and Muzaffarpur districts was adversely affected (Figure 9 *a*). The impact of floods varied significantly among the districts, with Darbhanga having the highest total flood-affected agricultural land (84,302.58 ha) and the highest population affected (1,382,250), while Kishanganj had the lowest total flood-affected agricultural land (2,903.59 ha) and the lowest population (30,596) affected[29,30].

Flood 2021

The analysis showed that the 2021 flood events occurred in four phases. The first phase was in the last week of June 2021, the second phase in the first week of July 2021, the third phase in the first week of August 2021 and the fourth phase in the last week of August 2021. It was also observed that the extent of flooded areas varied significantly across the districts, from 2,970 ha in Sheohar to 86,790 ha in Bhagalpur. The number of people affected by the floods also varied significantly, from 44,155 in Sheohar to 1,219,906 in Darbhanga (Figure 9 *b*). Some districts, such as Bhagalpur, Katihar, Darbhanga and Muzaffarpur, experienced large flooded areas and high population displacement. Other districts, such as Gopalganj, Sheohar, Siwan and Supaul, had smaller flooded areas but still had a considerable number of people affected by the floods.

Accuracy assessment and validation of results

The accuracy of the extracted flood extent areas was validated independently using datasets that included high-resolution satellite images from Google Earth and the flood extent layer of National Remote Sensing Centre (NRSC)[31]. Validation points were carefully selected to ensure representation across the entire image. Approximately 260 validation points were chosen within the study area. Subsequently, confusion matrices were generated to assess the classification performance, a commonly employed method for multi-class classification evaluations[32]. The overall accuracy obtained exceeded 89%, thereby confirming the suitability of the Otsu automatic thresholding method for rapid and efficient flood mapping[22].

In addition to the aforementioned validation datasets, the advisory document from the State Disaster Management Authority (SDMA) and data from the Flood Management Information System, Bihar and the crop area affected report of NRSC[33] were employed to further validate the study. This comprehensive validation approach, which involved multiple independent sources, strengthens the credibility of the results of this study.

Conclusion

In this study, the impact of floods on agriculture in North Bihar has been assessed. Optical remote sensing data, Sentinel-2 and PlanetScope, hosted on GEE cloud platform, have been used to delineate pre- and post-flood land-use

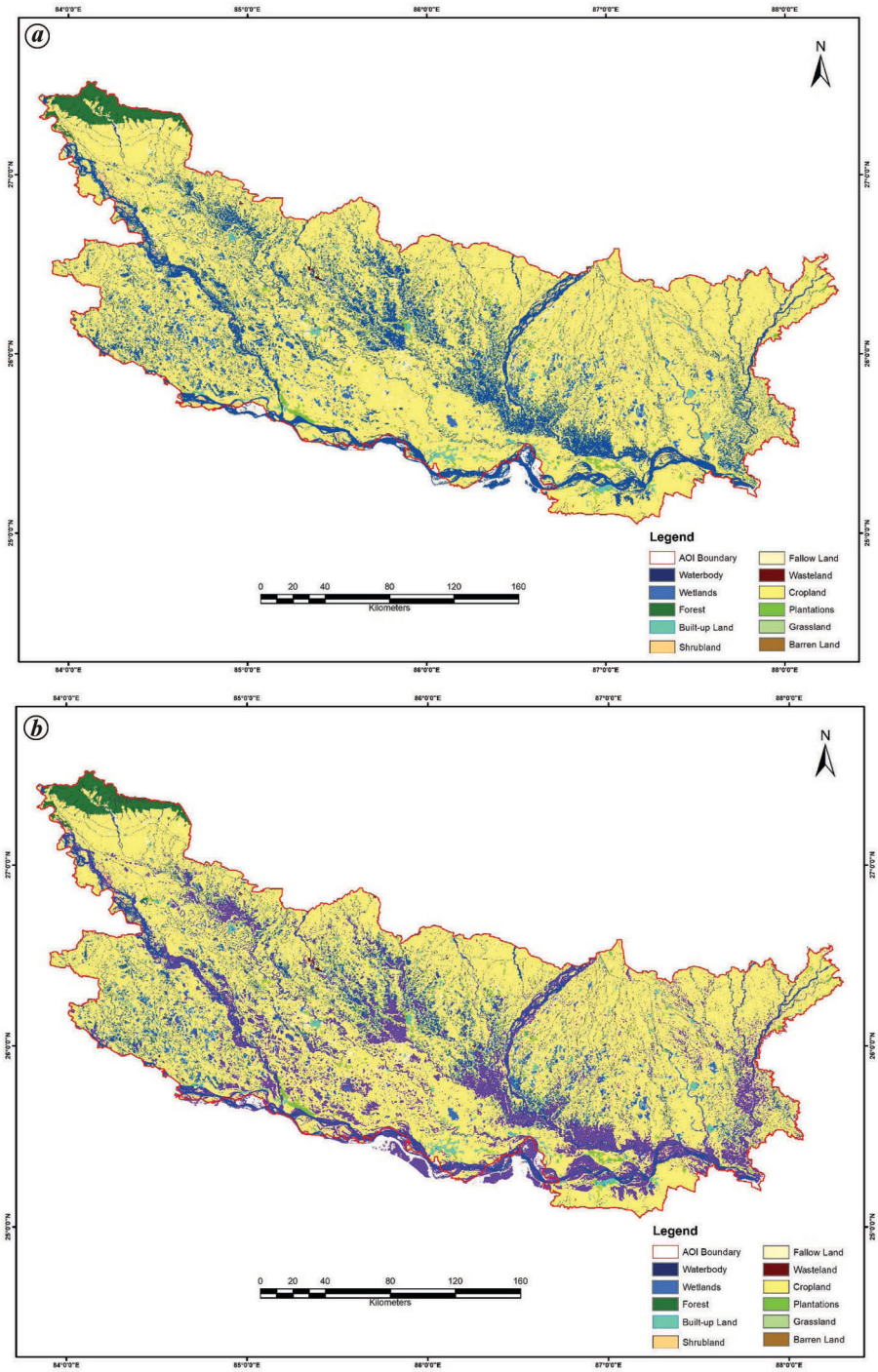

Figure 9. Flood-affected land-use map of (***a***) 2020 and (***b***) 2021.

maps for 2020 and 2021. Sentinel-1 SAR data were used to identify flood pixels employing the automated thresholding technique on GEE. A JavaScript code was developed for processing the enormous datasets hosted on the GEE cloud computer platform within a short period. This code is capable of robust flood mapping and monitoring using microwave (SAR) satellite datasets on a large scale. It has been observed that about ~ 12.63% (701,967 ha) of the study area was flooded in 2020, while in 2021, about ~17.20% (955,897 ha) of the study area was flooded. The districts most affected by floods in 2021 were Bhagalpur, Darbhanga, Katihar, Muzaffarpur and Gopalganj. In 2021, about 4% more area of North Bihar was flooded compared to the floods of 2020. The results of this study have been validated using the flood extent layer generated by NRSC and the advisory document of SDMA, Bihar. It is expected that

the generated flood extent maps and area of statistics will be beneficial for the policymakers in future planning.

1. Freer, J., Beven, K., Neal, J., Schumann, G., Hall, J. and Bates, P., Flood risk and uncertainty. In *Risk and Uncertainty Assessment for Natural Hazards* (eds Rougier, J., Sparks, S. and Hill, L.), Cambridge University Press, Cambridge, 2013, pp. 190–233; https://doi.org/10.1017/CBO9781139047562.008.
2. Kumar, H., Karwariya, S. K. and Kumar, R., Google earth engine-based identification of flood extent and flood-affected paddy rice fields using Sentinel-2 MSI and sentinel-1 SAR data in Bihar state, India. *J. Indian Soc. Remote Sensing*, 2022; https://doi.org/10.1007/s12524-021-01487-3.
3. Torres, R., Snoeij, P., Geudtner, D., Bibby, D., Davidson, M., Attema, E., Potin, P. and Traver, I. N., GMES Sentinel-1 mission. *Remote Sensing Environ.*, 2012, **120**, 9–24; https://doi.org/10.1016/j.rse.2011.05.028.
4. Schumann, G. J., Brakenridge, G. R., Kettner, A. J., Kashif, R. and Niebuhr, E., Assisting flood disaster response with earth observation data and products: a critical assessment. *Remote Sensing*, 2018, **10**(8), 1230; https://doi.org/10.3390/rs10081230.
5. Ghosh, S., Kumar, D. and Kumari, R., Evaluating the impact of flood inundation with the cloud computing platform over vegetation cover of Ganga Basin during COVID-19. *Spat. Inf. Res.*, 2022, **30**, 291–308; https://doi.org/10.1007/s41324-022-00430-z.
6. Chini, M., Hostache, R., Giustarini, L. and Matgen, P., A hierarchical split-based approach for parametric thresholding of SAR images: flood inundation as a test case. *IEEE Trans. Geosci. Remote Sensing*, 2017, **55**(12), 6975–6988; https://doi.org/10.1109/TGRS.2017.2737664.
7. McFeeters, S. K., The use of the normalized difference water index (NDWI) in the delineation of open water features. *Int. J. Remote Sensing*, 1996, **17**(7); 1425–1432; https://doi.org/10.1080/01431169608948714.
8. Xu, H., Modification of normalized difference water index (NDWI) to enhance open water features in remotely sensed imagery. *Int. J. Remote Sensing*, 2006, **27**(14), 3025–3033; https://doi.org/10.1080/01431160600589179.
9. Feyisa, G. L., Meilby, H., Fensholt, R. and Proud, S. R., Automated water extraction index: a new technique for surface water mapping using Landsat imagery. *Remote Sensing Environ.*, 2014, **140**, 23–35; https://doi.org/10.1016/j.rse.2013.08.029.
10. Ray, K., Pandey, P., Pandey, C., Dimri, A. P. and Kishore, K., On the recent floods in India. *Curr. Sci.*, 2019, **117**(2), 204–218.
11. Bhatt, C. M., Gupta, A., Roy, A., Dalal, P. and Chauhan, P., Geospatial analysis of September, 2019 floods in the Lower Gangetic Plains of Bihar using multi-temporal satellites and river gauge data. *Geomat. Natural Haz. Risk*, 2020, **12**, 84–102; https://doi.org/10.1080/19475705.2020.1861113.
12. Anusha, N. and Bharathi, B., Flood detection and flood mapping using multi-temporal synthetic aperture radar and optical data. *Egypt. J. Remote Sensing Space Sci.*, 2020, **23**, 207–219.
13. Khan, A., Govil, H., Khan, H. H., Kumar Thakur, P., Yunus, A. P. and Pani, P., Channel responses to flooding of Ganga River, Bihar India, 2019 using SAR and optical remote sensing. *Adv. Space Res.*, 2021; https://doi.org/10.1016/j.asr.2021.08.039.
14. Jeganathan, C. and Kumar, P., Mapping agriculture dynamics and associated flood impacts in Bihar using time-series satellite data. *Climate Change Agric. India: Impact Adaptation*, Springer, Cham., 2018; https://doi.org/10.1007/978-3-319-90086-5_5.
15. Government of India (GoI), Census of India, 2011; https://censusindia.gov.in/2011-prov-results/data_files/bihar/Provisional%20Population%20Totals%202011-Bihar.pdf (accessed on 10 March 2022).
16. GoI, Department of Agriculture, Cooperation and Farmers' Welfare, 2020; https://farmech.dac.gov.in/FarmerGuide/BI/1.htm (accessed on 5 January 2023).
17. Vizzari, M., PlanetScope, Sentinel-2, and Sentinel-1 data integration for object-based land cover classification in Google Earth Engine. *Remote Sensing*, 2022, **14**(11), 2628; https://doi.org/10.3390/rs14112628.
18. Pascual, A., Tupinambá-Simões, F., Guerra-Hernández, J. and Bravo, F., High-resolution planet satellite imagery and multi-temporal surveys to predict risk of tree mortality in tropical eucalypt forestry. *J. Environ. Manage.*, 2022, **310**, 114804.
19. Arif, F. and Akbar, M., Resampling air borne sensed data using bilinear interpolation algorithm. In IEEE International Conference on Mechatronics, ICM'05, Taipei, Taiwan, 2005, pp. 62–65; doi:10.1109/ICMECH.2005.1529228.
20. Xia, M., Li, S., Chen, W. and Yang, G., Perceptual image hashing using rotation invariant uniform local binary patterns and color feature. In *Advances in Computers*, 2023, vol. 130, pp. 163–205; https://doi.org/10.1016/bs.adcom.2022.12.001.
21. Otsu, N., A threshold selection method from gray-level histograms. *IEEE Trans. Syst, Man Cybern.*, 1979, **9**(1), 62–66.
22. Kordelas, G., Manakos, I., Aragones, D. G., Díaz-Delgado, R. and Bustamante, J., Fast and automatic data-driven thresholding for inundation mapping with Sentinel-2 data. *Remote Sensing*, 2018, **10**, 910.
23. Moharrami, M., Javanbakht, M. and Attarchi, S., Automatic flood detection using Sentinel-1 images on the Google Earth Engine. *Environ. Monit. Assess.*, 2021, **193**, 248; https://doi.org/10.1007/s10661-021-09037-7.
24. Xue, J. and Zhang, Y., Ridler and Calvard's, Kittler and Illingworth's and Otsu's methods for image thresholding. *Pattern Recogn. Lett.*, 2012, **33**, 793–797.
25. Manjusree, P., Prasanna Kumar, L., Bhatt, C. M., Rao, G. S. and Bhanumurthy, V., Optimization of threshold ranges for rapid flood inundation mapping by evaluating backscatter profiles of high incidence angle SAR images. *Int. J. Disaster Risk Sci.*, 2012, **3**, 113–122.
26. Liang, J. and Liu, D., A local thresholding approach to flood water delineation using Sentinel-1 SAR imagery. *ISPRS J. Photogramm. Remote Sensing*, 2020, **159**, 53–62; https://doi.org/10.1016/J.ISPRSJPRS.2019.10.017.
27. Central Water Commission, Daily flood situation report cum advisories, GoI, New Delhi, 2020; http://cwc.gov.in/fmo/dfsra
28. Central Water Commission. Daily flood situation report cum advisories, GoI, New Delhi, 2021; http://cwc.gov.in/fmo/dfsra
29. State Disaster Management Department, Bihar; http://disastermgmt.bih.nic.in/cumulative%20flood%20report%202020/cum05092020.pdf (accessed on 5 January 2023).
30. Flood Management Information System, Bihar, 2020.
31. NRSC, Cumulative Flood Inundated areas of Bihar State (9 to 23 July 2020).
32. Olofsson, P., Foody, G. M., Herold, M., Stehman, S. V., Woodcock, C. E. and Wulder, M. A., Good practices for estimating area and assessing accuracy of land change. *Remote Sensing Environ.*, 2014, **148**, 42–57.
33. NRSC, Cropped area affected due to flooding in Bihar state (based on flood layer from July 3 to 7 August 2020) dated 19.08.2020, Map no. 2020/92, NRSC/ISRO, Hyderabad.

Received 26 March 2023; revised accepted 18 July 2023

doi: 10.18520/cs/v125/i8/886-895